Polymer Chemistry

ROYAL SOCIETY OF CHEMISTRY

COMMUNICATION

Check for updates

Self-catalyzing photoredox polymerization for recyclable polymer catalysts†

Jacob J. Lessard,‡ Georg M. Scheutz,‡ Angie B. Korpusik, Rebecca A. Olson, C. Adrian Figg [ID] * and Brent S. Sumerlin [ID] *

We describe a self-catalyzing photoredox polymerization system for the modular generation of macromolecular photocatalysts. Specifically, we designed a photoactive eosin Y-derived monomer that can induce photoelectron/energy transfer, while simultaneously partaking in reversible addition–fragmentation chain transfer polymerization as a monomer, affording polymer catalysts with tunable eosin Y incorporations.

Photoredox catalysis has emerged as a powerful technique in organic and polymer synthesis.[1–5] Specifically, recyclable catalyst systems are desirable due to improved reagent economy and sustainability.[6–15] In this report, we describe the development of a modular self-catalyzing photoredox polymerization system that affords macromolecular photocatalysts for homogenous reaction conditions.

Previous strategies for recyclable photocatalytic vinyl polymerizations have focused on heterogeneous systems.[6–10] A potential drawback of heterogenous catalysis in light-mediated reaction systems is impaired light penetration through the reaction solution, which can lower the reaction efficiency.[11] Homogeneous catalysis can alleviate such problems by providing better access to catalytically active sites and improved light penetration for all reaction components.[16] However, separation of the homogenously dissolved catalyst from the reaction mixture for recycling is challenging.

We designed a novel, photoactive eosin Y (EY)-derived methacrylate monomer, denoted here as eosin Y methacrylate (EYMA), that can mediate trithiocarbonate reversible addition–fragmentation chain transfer (RAFT)[17,18] agents *via* a photoelectron/energy transfer (PET).[5,19–21] We hypothesized that as EYMA is incorporated into the polymer, the photoactive EY

xanthene moiety will continue to activate the RAFT agent in a self-catalytic process, where the reaction product (*i.e.*, the copolymer comprising EYMA) catalyzes the polymerization (Fig. 1). EY is also commonly used in other photoredox reactions[22,23] providing a modular platform for the generation of metal-free polymeric photocatalysts, where the nature of the polymer can be easily tuned by the selection of the comonomer, the monomer feed ratio, and the molecular weight. We believe that this strategy will substantially improve future development of individually designed and optimized photocatalyst systems for various reaction conditions.

Results and discussion

Monomer catalyst

We envisioned using a photocatalyst-functional monomer with a polymerizable vinyl group, allowing for simultaneous photoredox activation and incorporation *via* propagation into the polymer chain. For this purpose, we synthesized EYMA by tethering EY to 2-hydroxyethyl methacrylate using carbodiimide coupling (Fig. S1–5†). Since esterification of the 2-xanthenyl benzoic acid group could potentially affect the photophysical properties,[24] we also synthesized the model compound eosin Y methyl ester (EYMe) lacking a polymeriz-

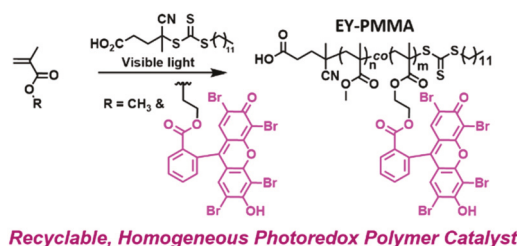*Recyclable, Homogeneous Photoredox Polymer Catalyst*

Fig. 1 Reaction scheme for the self-catalyzed photoredox polymerization of methyl methacrylate and the eosin Y-derived methacrylate under visible light (yellow or green) affording the polymeric catalyst EY-PMMA.

George & Josephine Butler Polymer Research Laboratory, Center for Macromolecular Science & Engineering, Department of Chemistry, University of Florida, Gainesville, Florida 32611, USA. E-mail: adrian_figg@northwestern.edu, sumerlin@chem.ufl.edu

†Electronic supplementary information (ESI) available: Materials, instrumentation, monomer synthesis, polymerizations, and catalysis. See DOI: 10.1039/d1py00208b

‡These authors contributed equally.

able vinyl group as a control. UV-vis spectroscopy of EYMe and EYMA showed little to no change in the visible light absorbance compared to EY (Fig. S6†), suggesting that EYMA has photoredox properties similar to EY.

Typically, EY-catalyzed polymerizations are performed with light irradiation close to the maximum absorbance of EY ($\lambda_{\max}$ ≈ 540 nm), allowing for efficient photoredox activation at low catalyst loadings.[20,25] While limiting the amount of catalyst is usually desirable, we sought to use high photocatalyst loadings to achieve increased EYMA incorporations into the resulting polymer to minimize the amount of the resulting macromolecular catalyst that would be needed in subsequent photocatalyzed reactions. Therefore, we used yellow light irradiation ($\lambda_{\max}$ = 595 nm) with an emission that overlaps only slightly with the absorbance of the EY derivatives to improve the light penetration and limit the number of activated species to accommodate such high photocatalyst loadings.

Polymerizations using EY, EYMe, and EYMA were conducted to test the use of yellow light on EY-catalyzed PET-RAFT polymerizations and to further understand the effect of catalyst conjugation. PET-RAFT polymerizations of methyl methacrylate (MMA) were conducted using each photocatalyst (0.1 : 1 catalyst : RAFT agent) in DMSO (Fig. 2). We discovered similar kinetic profiles with apparent rate constants for polymerization (k_{app}) ranging from 0.35 to 0.43 h^{-1}, suggesting that esterification and incorporation of EY into the polymer had little effect on catalytic efficiency. In all of these reactions, 4-(dimethylamino)pyridine (DMAP) was used as an electron donor[25,26] to limit photobleaching of the catalyst (Fig. S7†).

Having ensured the reactivity of EYMA was akin to EY, we conducted self-catalyzed photoredox copolymerizations of MMA with EYMA at varying feed ratios under yellow light irradiation (Fig. 3). The copolymerizations were conducted at 0.01, 0.1, and 1 equiv. EYMA with respect to RAFT agent (Fig. 3A, B & S8, 9†). Upon increasing the EYMA loading from
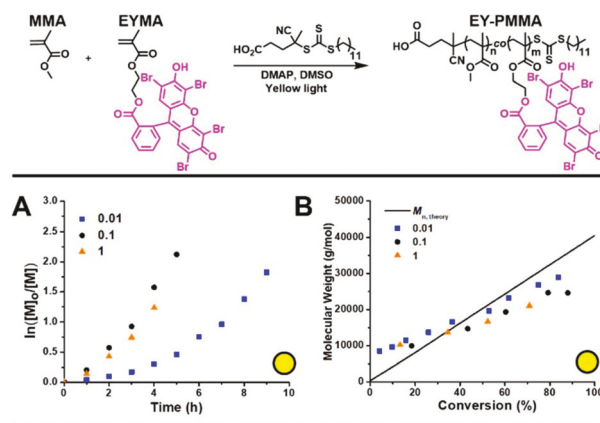

Fig. 3 Self-catalyzed photoredox copolymerizations of MMA and EYMA. (A) Pseudo-first-order rate plot and (B) number average molecular weight (M_n) versus conversion of the self-catalyzed photoredox copolymerization of MMA (400 equiv. to RAFT agent) and EYMA at 0.01 (blue), 0.1 (black), and 1 (orange) equiv with respect to RAFT agent under yellow light irradiation. M_n was obtained via conventional calibration relative to poly(methyl methacrylate) (PMMA) standards.

0.01 to 0.1 equiv., we observed a substantial polymerization rate increase. However, little difference was observed between 0.1 and 1 equiv. ($k_{app, \, 0.1 \, equiv.}$ = 0.43 h^{-1} & $k_{app, \, 1 \, equiv.}$ = 0.31 h^{-1}), likely due to a decreased light penetration from absorption at such high catalyst loadings. At the early stages of the polymerization, we recorded molecular weights higher than the theoretical values, which we attributed to slow activation of the RAFT agent. The number-average molecular weights obtained from size-exclusion chromatography (SEC) of all three EYMA loadings increased linearly with conversion, exhibiting final dispersity ($Đ$) values at or below 1.5. Later in the polymerization, molecular weights lower than the theoretical values were observed, which we believe is due to additional chain-transfer reactions involving the xanthene-core
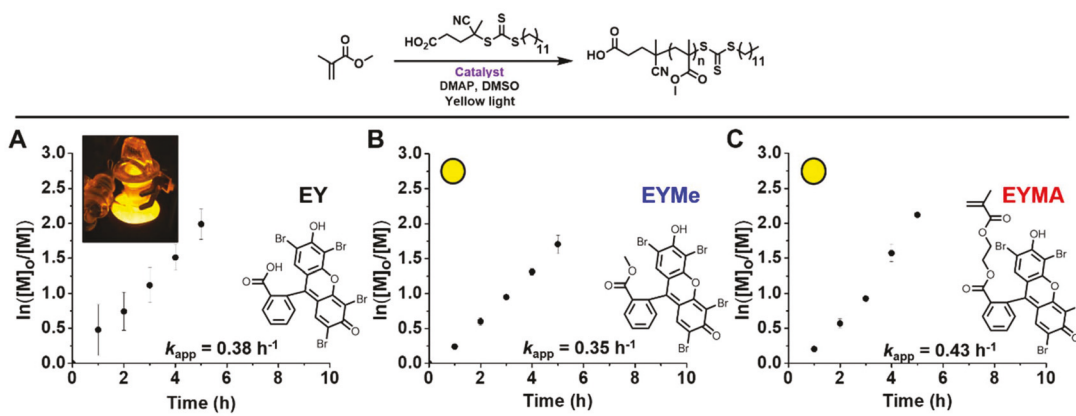

Fig. 2 Scheme and pseudo-first-order rate plots of the photoredox polymerization of MMA (400 equiv. to RAFT agent) with (A) EY, (B) EYMe, and (C) EYMA (all 0.1 equiv. to RAFT agent) under yellow light irradiation. The polymerizations were conducted at 5 M monomer concentration in DMSO with 1 equiv. of 4-(dimethylamino)pyridine (DMAP). All reactions were run in triplicate, and the averaged results are displayed with error bars corresponding to the standard deviation from the mean.

of EYMA. The evolution of molecular weight with conversion showed characteristics of slow RAFT agent consumption and possible chain-transfer, and these characteristics were also observed in green light-initiated polymerization with and without DMAP (Fig. S7, S10 and 11†). Ensuring that EYMA was incorporated into the polymers, UV-vis detection during SEC displayed a strong absorbance at 532 nm – indicative of EY being affixed to the polymer backbone (Fig. S12–23 & Table S1†).

Finally, we determined the total amount of EYMA in the purified EY-PMMA polymers by UV-vis spectroscopy (Fig. S24†), revealing EYMA incorporations lower than the feed ratio, which could be due to either a more sluggish polymerization of the bulky EYMA compared to MMA, or catalyst bleaching (Table S2†).

Polymer catalyst

To test whether the catalytic activity of EY is retained following polymerization, we conducted model photoredox reactions using the EY-PMMA as a catalyst. Specifically, we used EY-PMMA in the aerobic oxidative hydroxylation of 4-methoxyphenylboronic acid to the corresponding 4-methoxyphenol (Fig. 4). Phenols are versatile building blocks for polymers and pharmaceuticals,[27] and the development of efficient photocatalytic routes to this structural motif has recently gained increased attention.[28–33] Under reaction conditions adopted from Scaiano and coworkers,[30] EY-PMMA combined with diisopropylethylamine (i-Pr$_2$NEt) as an electron donor yielded 4-methoxyphenol with high conversion (>97%) at a catalyst loading of 2 mol% EY (incorporated in EY-PMMA) in 10 h open to air under green light irradiation (Fig. 4 & S25†). This result is on par with previous reports of photocatalytic oxidations of phenylboronic acids,[29,30,34] suggesting that the catalytic activity of EY-PMMA is comparable to that of small mole-

cule photocatalysts. An advantage of using polymeric catalysts is that the polymer can be readily retrieved using common precipitation techniques. We were able to recover over 98 wt% of the catalytic polymer after precipitation into diethyl ether. The recovered EY-PMMA was used in two additional oxidative hydroxylation reaction cycles, maintaining a final conversion above 97%, indicating good catalyst stability (Fig. 4 & S26†). Furthermore, SEC and ^{1}H NMR analysis of EY-PMMA after three reaction-precipitation cycles showed no significant change of molecular weight and composition; however, a slight decrease in catalyst recovery was observed over recycling studies (Fig. S27–29†).

To further demonstrate the versatility and the recyclability of EY-PMMA, we used the polymer catalyst, recovered after the three cycles of 4-methoxyphenyl boronic acid oxidation, to perform a photoredox polymerization of hexyl methacrylate (HMA) under green light (Fig. 5). After the polymerization, EY-PMMA was removed from poly(hexyl methacrylate) (PHMA) by precipitation into cold hexanes, yielding a final catalyst recovery of 44 wt% (Fig. S30†). PHMA was analyzed by SEC and ^{1}H NMR spectroscopy, showing excellent agreement between theoretical and experimental molecular weight and all the expected characteristic proton signals (Fig. 5 & S31†). Additionally, SEC coupled with a UV-vis detector at 532 nm verified complete removal of EY-PMMA from PHMA (Fig. S32†). Excitingly, all four reactions displayed complete removal of the photocatalyst and give a sense of the vast array of conditions and types of transformations capable with these tailored polymer photocatalyst systems.

Lastly, to validate that self-catalyzing photoredox polymerization can be employed in a variety of different polymerization conditions and for the generation of functional materials, we synthesized polymeric nanoparticles *via* self-catalyzing
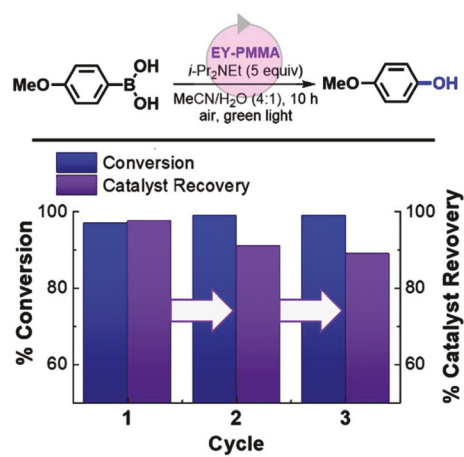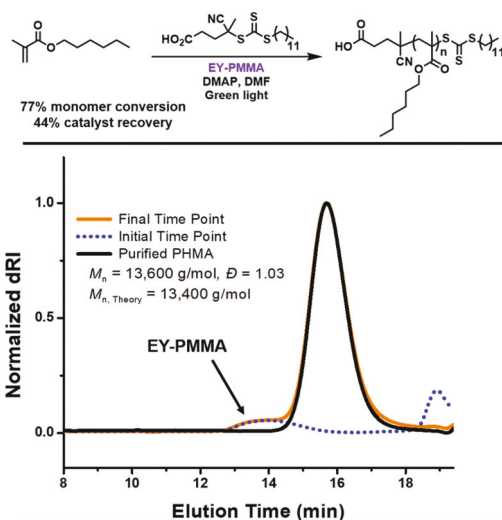
Fig. 4 Reaction scheme for the photo-mediated oxidation of 4-methoxyphenyl boronic acid to 4-methoxyphenol using EY-PMMA with diisopropylethylamine (i-Pr$_2$NEt) open to air under green light (top). Constant conversion and good catalyst recovery over three consecutive reaction-precipitation cycles indicate good recyclability (bottom).

Fig. 5 Polymerization of hexyl methacrylate using recycled EY-PMMA. SEC of the reaction solution before (blue dashed line), after polymerization (orange), and after purification (black) showing complete removal of the EY-PMMA catalyst (M_n and dispersity ($Đ$) determined by SEC equipped with multi-angle light scattering detection).
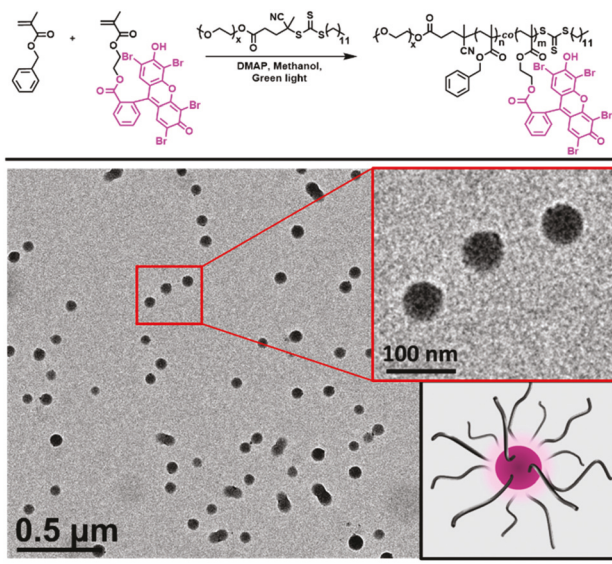
Fig. 6 Formation of micelles *via* self-catalyzing polymerization-induced self-assembly. Transmission electron microscopy image of poly (ethylene glycol)-*block*-poly(eosin Y methacrylate-*co*-benzyl methacrylate) micelles with a representative cartoon depiction of a dye labeled micelle in the inset.

polymerization-induced self-assembly (PISA). Using EYMA and benzyl methacrylate (BnMA) in methanol with a polyethylene glycol (PEG) macro-RAFT agent, spherical micelles were formed under green light irradiation (Fig. 6 & S33, 34†). Considering these results, we believe that this approach bears great potential for the facile construction of polymer assemblies with dye-labeled cores, which could find application in sensing, imaging, or phototherapy.[35–37]

Conclusions

The described strategy holds great promise for the modular generation of tailor-made recyclable catalysts for homogenous reaction conditions while maintaining facile catalyst recovery. The ability for the EYMA to self-catalyze under visible light irradiation, both as a monomer and while incorporated into the polymer chain, affords macromolecular catalysts under mild reaction conditions. Importantly, the catalytic activity and recyclability of the polymeric photocatalyst was retained following polymerization, demonstrated by photo-mediated oxidative hydroxylation reactions, PET-RAFT polymerizations of hexyl methacrylate, and self-catalyzed PISA. This approach allows for individual optimization of photocatalyst design parameters under mild reaction conditions, a template which has significant potential for future homogenous-to-heterogenous catalyst systems.

Conflicts of interest

The authors declare no competing financial interest.

Notes and references

1 C. K. Prier, D. A. Rankic and D. W. C. MacMillan, *Chem. Rev.*, 2013, **113**, 5322–5363.
2 N. A. Romero and D. A. Nicewicz, *Chem. Rev.*, 2016, **116**, 10075–10166.
3 M. Chen, M. Zhong and J. A. Johnson, *Chem. Rev.*, 2016, **116**, 10167–10211.
4 T. G. McKenzie, Q. Fu, M. Uchiyama, K. Satoh, J. Xu, C. Boyer, M. Kamigaito and G. G. Qiao, *Adv. Sci.*, 2016, **3**, 1500394.
5 N. Corrigan and C. Boyer, *ACS Macro Lett.*, 2019, **8**, 812–818.
6 M. Chen, S. Deng, Y. Gu, J. Lin, M. J. MacLeod and J. A. Johnson, *J. Am. Chem. Soc.*, 2017, **139**, 2257–2266.
7 S. Shanmugam, S. Xu, N. N. M. Adnan and C. Boyer, *Macromolecules*, 2018, **51**, 779–790.
8 Y. Chu, N. Corrigan, C. Wu, C. Boyer and J. Xu, *ACS Sustainable Chem. Eng.*, 2018, **6**, 15245–15253.
9 X. Li, Y. C. Zhang, Y. Zhao, H. P. Zhao, B. Zhang and T. Cai, *Macromolecules*, 2020, **53**, 1550–1556.
10 K. P. McClelland, T. D. Clemons, S. I. Stupp and E. A. Weiss, *ACS Macro Lett.*, 2019, **9**, 7–13.
11 X. Yu and S. M. Cohen, *Chem. Commun.*, 2015, **51**, 9880–9883.
12 T. Zhang, W. Liang, Y. Huang, X. Li, Y. Liu, B. Yang, C. He, X. Zhou and J. Zhang, *Chem. Commun.*, 2017, **53**, 12536–12539.
13 J.-X. Jiang, Y. Li, X. Wu, J. Xiao, D. J. Adams and A. I. Cooper, *Macromolecules*, 2013, **46**, 8779–8783.
14 J. D. Smith, A. M. Jamhawi, J. B. Jasinski, F. Gallou, J. Ge, R. Advincula, J. Liu and S. Handa, *Nat. Commun.*, 2019, **10**, 1837.
15 Q. Cao, J. Barrio, M. Antonietti, B. Kumru, M. Shalom and B. V. K. J. Schmidt, *ACS Appl. Poly. Mater.*, 2020, **2**, 3346–3354.
16 D. J. Cole-Hamilton, *Science*, 2003, **299**, 1702.
17 M. R. Hill, R. N. Carmean and B. S. Sumerlin, *Macromolecules*, 2015, **48**, 5459–5469.
18 S. Perrier, *Macromolecules*, 2017, **50**, 7433–7447.
19 C. Wu, N. Corrigan, C.-H. Lim, K. Jung, J. Zhu, G. Miyake, J. Xu and C. Boyer, *Macromolecules*, 2019, **52**, 236–248.
20 J. Phommalysack-Lovan, Y. Chu, C. Boyer and J. Xu, *ChemComm*, 2018, **54**, 6591–6606.
21 M. L. Allegrezza and D. Konkolewicz, RAFT Polymerization: Mechanistic Perspectives for Future Materials, *ACS Macro Lett.*, 2021, **10**, 433–446.
22 D. Ravelli, M. Fagnonia and A. Albini, *Chem. Soc. Rev.*, 2013, **42**, 97–113.

23 V. Srivastavaa and P. P. Singh, *RSC Adv.*, 2017, **7**, 31377–31392.

24 J. C. del Valle, J. Catalán and F. Amat-Guerri, *J. Photochem. Photobiol., A*, 1993, **72**, 49–53.

25 C. A. Figg, J. D. Hickman, G. M. Scheutz, S. Shanmugam, R. N. Carmean, B. S. Tucker, C. Boyer and B. S. Sumerlin, *Macromolecules*, 2018, **51**, 1370–1376.

26 J. Xu, S. Shanmugam, H. T. Duong and C. Boyer, *Polym. Chem.*, 2015, **6**, 5615–5624.

27 J.-F. Lutz, D. Neugebauer and K. Matyjaszewski, *J. Am. Chem. Soc.*, 2003, **125**, 6986–6993.

28 K. Ohkubo, T. Kobayashi and S. Fukuzumi, *Angew. Chem., Int. Ed.*, 2011, **50**, 8652–8655.

29 Y. Q. Zou, J. R. Chen, X. P. Liu, L. Q. Lu, R. L. Davis, K. A. Jorgensen and W. J. Xiao, *Angew. Chem., Int. Ed.*, 2012, **51**, 784–788.

30 S. P. Pitre, C. D. McTiernan, H. Ismaili and J. C. Scaiano, *J. Am. Chem. Soc.*, 2013, **135**, 13286–13289.

31 H. Wang, W. G. Li, K. Zeng, Y. J. Wu, Y. Zhang, T. L. Xu and Y. Chen, *Angew. Chem., Int. Ed.*, 2019, **58**, 561–565.

32 X. Yan, H. Liu, Y. Li, W. Chen, T. Zhang, Z. Zhao, G. Xing and L. Chen, *Macromolecules*, 2019, **52**, 7977–7983.

33 H. M. Yang, M. L. Liu, J. W. Tu, E. Miura-Stempel, M. G. Campbell and G. J. Chuang, *J. Org. Chem.*, 2020, **85**, 2040–2047.

34 H. Y. Xie, L. S. Han, S. Huang, X. Lei, Y. Cheng, W. Zhao, H. Sun, X. Wen and Q. L. Xu, *J. Org. Chem.*, 2017, **82**, 5236–5241.

35 S. Kim and H. D. Sikes, *ACS Appl. Bio Mater.*, 2018, **1**, 216–220.

36 S. Kim and H. D. Sikes, *ACS Appl. Mater. Interfaces*, 2019, **11**, 28469–28477.

37 G. Liu, J. Hu, G. Zhang and S. Liu, *Bioconjugate Chem.*, 2015, **26**, 1328–1338.